Available online at www.sciencedirect.com
SCIENCE DIRECT
Biochimica et Biophysica Acta 1709 (2005) 69 – 83
BIOCHIMICA ET BIOPHYSICA ACTA
BBA
http://www.elsevier.com/locate/bba

Modulation of photosynthetic electron transport in the absence of terminal electron acceptors: Characterization of the *rbcL* deletion mutant of tobacco

Yagut Allahverdiyeva[a], Fikret Mamedov[b], Pirkko Mäenpää[a], Imre Vass[c], Eva-Mari Aro[a,*]

[a]*Department of Biology, Plant Physiology and Molecular Biology, Turku University, FIN-20014 Turku, Finland*
[b]*Department of Molecular Biomimetics, Uppsala University, Villavägen 6, S-752 36 Uppsala, Sweden*
[c]*Plant Biology Institute, Biological Research Center, H-6701 Szeged, PO-BOX 521 Hungary*

Received 29 March 2005; received in revised form 6 June 2005; accepted 8 June 2005
Available online 1 July 2005

Abstract

Tobacco *rbcL* deletion mutant, which lacks the key enzyme Rubisco for photosynthetic carbon assimilation, was characterized with respect to thylakoid functional properties and protein composition. The Δ*rbcL* plants showed an enhanced capacity for dissipation of light energy by non-photochemical quenching which was accompanied by low photochemical quenching and low overall photosynthetic electron transport rate. Flash-induced fluorescence relaxation and thermoluminescence measurements revealed a slow electron transfer and decreased redox gap between Q_A and Q_B, whereas the donor side function of the Photosystem II (PSII) complex was not affected. The 77 K fluorescence emission spectrum of Δ*rbcL* plant thylakoids implied a presence of free light harvesting complexes. Mutant plants also had a low amount of photooxidisible P700 and an increased ratio of PSII to Photosystem I (PSI). On the other hand, an elevated level of plastid terminal oxidase and the lack of F_0 'dark rise' in fluorescence measurements suggest an enhanced plastid terminal oxidase-mediated electron flow to O_2 in Δ*rbcL* thylakoids. Modified electron transfer routes together with flexible dissipation of excitation energy through PSII probably have a crucial role in protection of PSI from irreversible protein damage in the Δ*rbcL* mutant under growth conditions. This protective capacity was rapidly exceeded in Δ*rbcL* mutant when the light level was elevated resulting in severe degradation of PSI complexes.

Keywords: Photosynthesis; Photosystem II; Photosystem I; Photoinhibition; Rubisco

1. Introduction

Photosynthetic light reactions convert absorbed light energy into chemical energy (NADPH and ATP), which is primarily used for CO_2 fixation to form carbohydrates. Rubisco, the key enzyme of CO_2 fixation, is composed of eight Large Subunits, encoded by a single gene (*rbcL*) of the multicopy chloroplast genome and eight Small Subunits, encoded by a small multigene (*rbcS*) family in the nucleus [1]. In fact, Rubisco catalyses two competing reactions, both of which are the main consumers of the photosynthetically generated electrons: CO_2 fixation in photosynthesis and the production of 2-phosphoglycolate in the photorespiratory pathway. In this study, we used a tobacco *rbcL* deletion mutant, which lacks the large subunit of Rubisco [2], to investigate in vivo the effects of the deficiency of these two

Abbreviations: Chl, chlorophyll; CP29, CP26, minor light-harvesting complex proteins of PSII; Cyt, cytochrome; DAB, 3,3′-diaminobenzidine; DCMU, 3-(3,4-dichlorophenyl)-1,1-dimethylurea; DMBQ, 2,6-dimethyl-*p*-benzoquinone; EPR, electron paramagnetic resonance; ETR, electron transport rate; FNR, ferredoxin-NADP oxidoreductase; LHCII, major light-harvesting complex of PSII; NDH-1, proton-pumping NAD(P)H dehydrogenase 1 complex; Ndh-I, subunit of NDH-1 complex; NPQ, non-photochemical quenching; PQ, plastoquinone; PSI, Photosystem I; PSII, Photosystem II; P680, primary electron donor of PSII; P700, primary electron donor of PSI; Q_A and Q_B, the primary and secondary quinone acceptors in PSII; PTOX, plastid terminal oxidase; ROS, reactive oxygen species; Rubisco, ribulose-1,5-biphosphate carboxylase/oxygenase; TL, thermoluminescence; WT, wild type; Y_D, accessory tyrosine electron donor to P680, tyrosine 160 on the D2

* Corresponding author. Tel.: +358 2 333 5931; fax: +358 2 333 5549.
E-mail address: evaaro@utu.fi (E.-M. Aro).

0005-2728/$ - see front matter © 2005 Elsevier B.V. All rights reserved.
doi:10.1016/j.bbabio.2005.06.004

major electron consumers on the function and composition of the thylakoid membrane.

It is well known that conditions where the supply of light energy exceeds its utilization may lead to a decrease in photosynthetic activity and an irreversible photodamage to the photosynthetic apparatus [3]. A long-lasting debate in photosynthetic research has been the mechanisms of the photoinhibition of the photosynthetic apparatus. Indeed, it is well documented that the main target of photodamage is located in the Photosystem II (PSII) complex [4,5]. The central concept of PSII inactivation by visible light was related to the loss of acceptor side activity of the PSII complex [6]. The Photosystem I (PSI) complex has been regarded relatively resistant against photodamage. However, under certain environmental conditions such as moderate illumination at chilling temperatures, the PSI complex can be the main target of photoinhibition of the photosynthetic apparatus [7–10]. In this case, a highly reduced stromal side of the photosynthetic electron transfer chain leads to a direct reduction of ground-state oxygen ($^3O_2$) by PSI and subsequent production of superoxide in addition to other reactive oxygen species (ROS), such as hydrogen peroxide (H_2O_2), hydroxyl radicals (·OH) and singlet oxygen. This in turn induces photoinhibition of PSI, and may also be dangerous to PSII complexes [11].

Photosynthetic organisms have developed a number of protective mechanisms in order to avoid damage to the photosynthetic apparatus under excess light conditions. These include a regulation of light absorption and subsequent utilization of the absorbed light energy. Down regulation of PSII activity by low pH, high energy dissipation by nonphotochemical quenching (NPQ) [12], inactivation of PSII and also the D1 protein turnover have been considered as protection mechanisms of PSII [13]. Several mechanisms for protection of PSI from photoinhibition have also been proposed: a water–water cycle [14], the xanthophyll cycle [15], and the cycling of electrons around PSI [16,17]. In this study, we attempted to analyze at molecular level the acclimation of the photosynthetic apparatus of the tobacco Δ*rbcL* mutant to growth light condition and also to a sudden exposure of plants to high irradiance. Our results show that the lack of terminal electron acceptors leads to a multitude of effects that help to acclimate the plants to increased excitation pressure under growth conditions. However, under strong illumination conditions, an accelerated loss of both PSI and PSII activity occurs.

2. Materials and methods

2.1. Plant material, isolation of thylakoid membranes and chlorophyll determination

Tobacco wild type (WT) (*Nicotiana tabacum* cv Petit Havana) and Δ*rbcL* mutant plants were grown aseptically on MS-medium containing 3% sucrose [18] at 23 °C under a 16/8-h photoperiod of 10 μmol photons m^{-2} s^{-1} white light. The mature leaves from 6- to 8-week-old plants were used for experiments.

Thylakoid membranes were isolated from tobacco leaves with standard methods. Leaves were homogenized in ice-cold buffer containing 40 mM HEPES (pH 7.6), 5 mM $MgCl_2$, 10 mM NaCl, 2 mM EDTA, 0.4 M sucrose, and 1 g/L BSA, 1 g/L NaAsc. The homogenate was filtered through Miracloth and centrifuged for 10 min at 6000 g. The resulting pellet was washed with 10 mM HEPES pH 7.5, 5 mM $MgCl_2$, 10 mM NaCl and finally resuspended in 40 mM HEPES pH 7.5, 5 mM $MgCl_2$, 15 mM NaCl, and 0.4 M sucrose and stored at −80 °C until use.

Chlorophyll (Chl) was extracted in 80% (v/v) buffered acetone (2.5 mM HEPES–NaOH, pH 7.5) and quantified as described [19].

2.2. Photoinhibitory treatment

Unless otherwise stated, the in vivo photoinhibition was induced by illuminating plants at 1000 μmol photons m^{-2} s^{-1} of white light. Rapid thylakoid isolation was carried out immediately after the light treatment.

For in vitro photoinhibition isolated thylakoid membranes (100 mL, 10 μg Chl/mL) were illuminated at 300 μmol photons m^{-2} s^{-1} of white light in temperature controlled open glass containers at 25 °C. The samples were continuously stirred during the treatment. At given time points, the fluorescence measurements were performed. Thylakoid membranes were dark adapted for 5 min prior to fluorescence measurements.

2.3. Chl fluorescence

Non-photochemical quenching of Chl fluorescence in plants exposed to actinic red light (LED array max. 655 nm emission) of 120 μmol photons m^{-2} s^{-1} was determined using PAM-2000 Fluorometer and analyzed using the DATA Acquisition Software DA-2000 (Walz, Effeltrich, Germany). Plants were placed in the dark for at least 1 h prior to recording the dark level maximum (F_m) and minimal (F_0) fluorescence. The NPQ-parameter was calculated according to the equation: $NPQ=(F_m-F'_m)/F'_m$.

Photosynthetic electron transport rate (ETR) was calculated from Rapid Light Curves recorded with the MINI-PAM (Walz GmbH, Effeltrich, Germany) and plotted as a function of actinic irradiance. ETR=Yield* PAR*0.5*0.84, where 'Yield'—($\Delta F/F'_m$) represents the overall photochemical quantum yield, PAR is actinic irradiance in mol photons m^{-2} s^{-1}, 0.5 is a multiplication factor and the 0.84 standard factor is the incident quanta absorbed by the leaf.

Flash-induced increase and subsequent decay of Chl fluorescence yield was measured by a double-modulation

Fluorometer (P.S.I. Instruments, Brno). Samples, at 10 μg Chl mL^{-1}, were dark adapted for 5 min and Q_A^- reoxidation after a single saturating 10 μs flash, provided by red LED, was recorded in the 150 μs–100 s time range. Multi-component deconvolution of the relaxation curves was performed by using a fitting function with two exponential and one hyperbolic component as shown earlier [20]. The nonlinear correlation between the fluorescence yield and the redox state of Q_A was corrected for using the Joliot model [21] with a value of 0.5 for the energy-transfer parameter between PSII units.

The 'F_0 rise' measurement was performed using PAM101/103 Chlorophyll Fluorometer equipped with ED-101 unit. Detached leaves were illuminated with white actinic light at 100 μmol m^{-2} s^{-1} for 5 min prior dark transition.

77 K fluorescence emission spectra of thylakoid membranes were measured with a diode array spectrophotometer (S2000, Ocean Optics, Dunedin, Florida, USA) equipped with a reflectance probe as described [22]. Fluorescence was excited with light below 500 nm (defined with LS500S and LS700S filters, Corion Corp., Holliston, MA, placed in front of a slide projector) and the emission was recorded between 600 and 800 nm.

2.4. P700 oxido-reduction

P700 oxido-reduction in WT and Δ*rbcL* mutant leaves was assessed by monitoring the absorbance change at 820 nm using PAM 101/103 Fluorometer (Walz, Germany) equipped with ED-P700DW unit. The maximum content of photooxidisible P700 was determined using 532 nm single turnover flash (4 ns and an energy ~1.2 mJ/cm^2) provided from a Nd:YAG laser (Minilite, Continuum, Santa Clara, CA) and thylakoid membranes in the 0.5-mL reaction mixture containing 25 μg Chl in buffer consisting of 50 mM Tricine (pH 7.5), 5 mM $MgCl_2$, 15 mM NaCl, and 0.4 M sucrose.

2.5. Oxygen evolution measurements

Steady-state rates of oxygen evolution were measured using Hansatech DW1 O_2 electrode at saturating light intensity in the presence of 1 mM 2,6-dimethyl-*p*-benzoquinone (DMBQ) as an artificial electron acceptor. 1 mL thylakoid suspension at 10 μg Chl mL^{-1} was used in each measurement.

2.6. Thermoluminescence (TL) measurements

TL was measured with home-built apparatus as in [6]. Excitation of the samples was performed by Stroboslave (Radio General) Xenon flash of 0.5 mJ of 2 μs duration, at +5 °C in the absence or at −10 °C in the presence of the 10 μM 3-(3,4-dichlorophenyl)-1,1-dimethylurea (DCMU). After excitation, the samples immediately cooled down and the TL curves were recorded from −40 to + 80 °C at 20 °C min^{-1} heating rate.

2.7. EPR measurements

Room temperature EPR was measured with a Bruker Elexys E500 spectrometer equipped with a standard Bruker 4102 cavity as described in [23]. The relative amount of PSI in the thylakoid membranes was estimated from the intensity of non-saturated EPR spectra from chemically-oxidised $P700^+$. The relative amount of PSII was estimated from the intensity of non-saturated EPR spectra from the dark stable radical form $Y_D^{\cdot}$ of the D2 protein.

2.8. Pulse labeling of thylakoid proteins with [^{35}S] methionine

Leaf discs were pressed gently against coarse sandpaper to facilitate incorporation of [^{35}S] Met while floating on solution containing 30 μCi mL^{-1} of [^{35}S] Met in 0.4% (v/v) Tween 20. Leaves were pulse labeled for 1.5 h at irradiance of 30 μmol photons m^{-2} s^{-1}, followed by a chase at 500 μmol of photons m^{-2} s^{-1}. Before the chase, leaf discs were washed with 0.4% (v/v) Tween 20. After termination of pulse-chase labeling, the leaf discs were immediately frozen in liquid N_2 and the thylakoid membranes were isolated for autoradiography.

2.9. Gel electrophoresis, Western analysis, and autoradiography

SDS gel electrophoresis was carried out in 15% polyacrylamide gels with 6 M urea according to the method described by Laemmli [24]. For immunoblot analysis, the proteins were transferred to a PVDF membrane (Millipore) and immunodetection was performed using an ECL bioluminescence immunoblotting kit (Amersham, UK). For quantification, the immunoreactive bands were scanned with Fluorchem Image Analyzer (Alpha Innotech Corporation). For autoradiography, the gels were dried and exposed to X-ray films.

Blue-Native (BN) Polyacrylamide Gel Electrophoresis was performed according to [25] with some modifications [26]. After BN-PAGE the lanes were cut out, solubilised and laid on the top of SDS-PAGE to separate the protein subunits of the complexes. After electrophoresis, the proteins were visualised by silver staining.

2.10. H_2O_2 detection by 3,3′-diaminobenzidine (DAB) uptake method

H_2O_2 accumulation was detected by DAB-method [27]. Leaf discs from the high light treated leaves were placed in a solution containing 1% DAB (w/v) in 10 mM Mes (pH 5.8) for 1 h. Then, leaves were cleared by boiling in ethanol

(96%) for 5 min. H_2O_2 accumulation were visualised as a reddish-brown coloration.

3. Results

3.1. Phenotype of the ΔrbcL tobacco plant

Δ*rbcL* tobacco plants showed a clear phenotype even under low growth light conditions (~10 μmol photons m^{-2} s^{-1}) (Fig. 1). Compared with WT, the Δ*rbcL* plants were characterized by a slow growth rate and an elongated shape of the leaves. The Chl a/b ratio of Δ*rbcL* leaves was 2.6 compared to 3.1 in WT.

3.2. Photosynthetic ETR and NPQ

The whole chain photosynthetic ETR, calculated from Rapid Light Curves and plotted as a function of actinic irradiance in WT and Δ*rbcL* leaves is depicted in Fig. 2A. WT plants showed maximum ETR, ≈55 μmol electrons m^{-2} s^{-1}, at a PFD of 1090 μmol m^{-2} s^{-1}. Whereas Δ*rbcL* reached the maximal ETR, ≈14 μmol electrons m^{-2} s^{-1} already at low light, 135 μmol photons m^{-2} s^{-1}, with decline under higher irradiance.

The dissipation of light energy as heat in WT and Δ*rbcL* plants was monitored by measuring the development of NPQ during exposure of leaves to continuous actinic light. As shown in Fig. 2B, illumination of dark adapted WT leaves resulted in a fast development of large NPQ and approximately 25% of this quenching reversed during the first 4–5 min of actinic illumination. On the contrary, the Δ*rbcL* plants did not show the fast transient peak of NPQ typical to WT leaves, but instead showed an increasing NPQ with time, reaching a level of more than 2 times that of WT plants in 14 min. As shown from Fig. 2B, the dark relaxation of NPQ was fast in both WT and Δ*rbcL* leaves, implying that most of the NPQ observed in WT and Δ*rbcL* leaves can be ascribed to an energy-dependent quenching—qE [28]. Moreover, under continuous actinic light, WT leaves showed a strong photochemical quenching, whereas the mutant leaves showed extremely low photochemical quenching, suggesting that Q_A, the primary electron acceptor of PSII, remained largely reduced in mutant (data not shown).

3.3. Functional properties of the PSII complex in ΔrbcL plants

To elucidate the effects of the absence of terminal electron acceptors on the functional integrity of the PSII complex, we performed fluorescence, TL and oxygen evolution measurements with isolated thylakoid membranes and intact leaves. Fig. 3A shows a flash-induced increase and subsequent decay of the fluorescence yield in WT and Δ*rbcL* tobacco thylakoids. In the WT thylakoids, as also indicated previously [20], the fluorescence relaxation was dominated by the fast component (≈630 μs, 65%), arising from Q_A^- to Q_B electron transfer in PSII reaction centers, which had an oxidised or semireduced plastoquinone (PQ) molecule in the Q_B pocket at the time of flashing. The middle phase (≈22 ms, 16%), arises from Q_A^- reoxidation in

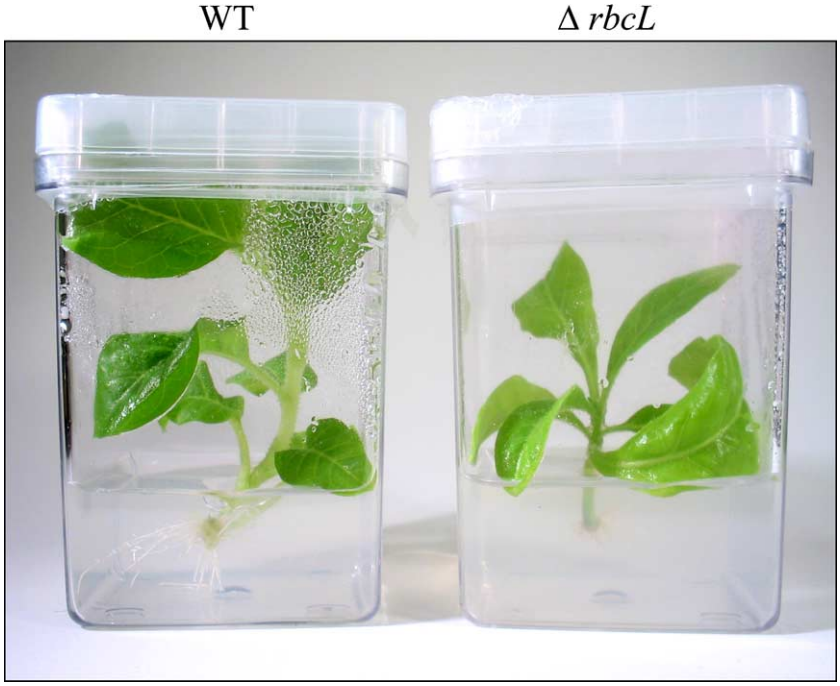

Fig. 1. Phenotype of WT and Δ*rbcL* tobacco plants. Plants were grown under 10 μmol m^{-2} s^{-1} photon flux.

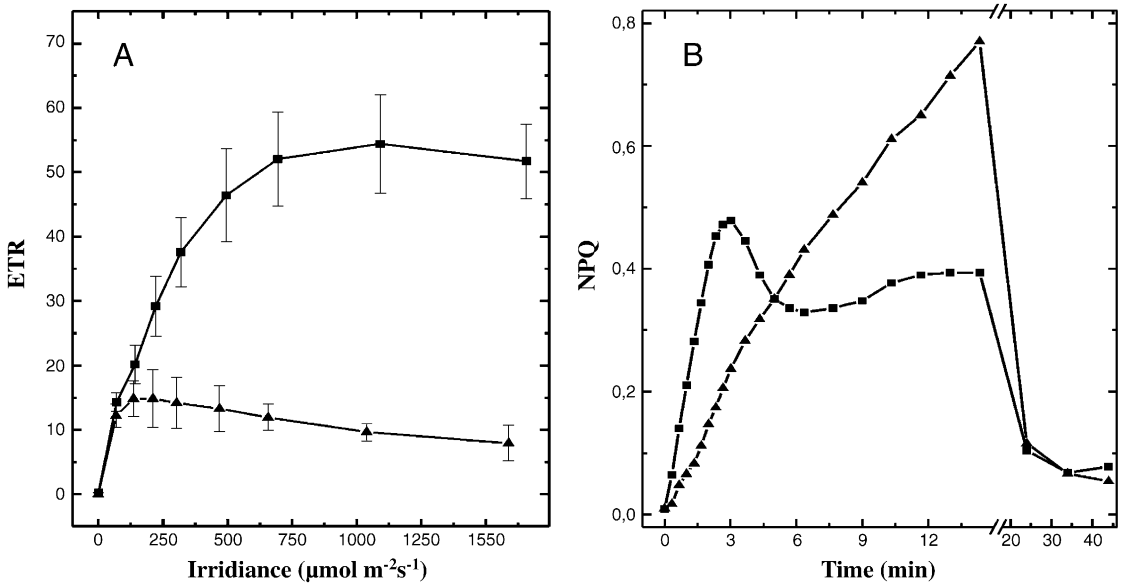

Fig. 2. Electron transport characteristics of the WT and Δ*rbcL* tobacco plants. (A) Light intensity dependence of the ETR in WT (squares) and Δ*rbcL* (triangles) leaves. The Rapid Light Curve consists of the fluorescence responses to nine different actinic irradiances of 10 s duration, separated by 0.8 s saturating pulse (2000 µmol photons m^{-2} s^{-1}). Each value represents mean of 4 experiments (±SD). (B) Light-induced development and subsequent dark relaxation of NPQ in WT (squares) and Δ*rbcL* (triangles) leaves. Dark adapted leaves were illuminated with ≈120 µmol photons m^{-2} s^{-1} of actinic red light for 14 min and then dark adapted further 30 min.

centers, which had an empty Q_B site in darkness and had to bind PQ from the pool. Finally, the slow phase of flash-induced fluorescence relaxation curve (≈9.3 s, 19%), shows the recombination of the S_2 state of the water oxidising complex with Q_B^- via the $Q_A^-Q_B \leftrightarrow Q_AQ_B^-$ equilibrium [29]. Comparative analysis of the kinetics of the flash-induced fluorescence relaxation showed that the fast (≈1.1 ms) and middle phases (≈29.6 ms) of the decay were significantly slowed down in Δ*rbcL* (Table 1). This indicates a modification in Q_A to Q_B electron transfer and a slower PQ binding to the Q_B pocket in Δ*rbcL* thylakoids as compared to WT. Moreover, in mutant thylakoids the relative amplitude of the fast relaxation phase decreased from 65% to 42%, with a concomitant increase in the relative amplitude of the middle phase from 16% to 19% as compared to WT (Table 1).

The slow phase of fluorescence relaxation, originating from $S_2(Q_AQ_B)^-$ recombination, showed in Δ*rbcL* thylakoids a faster time constant (5.9 s) and a dramatically larger amplitude (39%) compared to 9.3 s and 19%, respectively, in control WT thylakoids (Table 1).

In the presence of DCMU, which blocks the reoxidation of Q_A^- by forward electron transfer, the fluorescence relaxation indicates the status of the PSII donor side due to recombination of Q_A^- with donor side components. In a functional PSII complex, the recombination partner of Q_A^- is the S_2 state of the water oxidising complex. Interestingly, in the presence of DCMU, the overall fluorescence relaxation kinetics was identical in the WT and Δ*rbcL* thylakoid membranes (Fig. 3A, shown as inset and Table 1).

The above-described fluorescence measurements were performed in intact leaves as well. Fig. 3B shows the traces of flash-induced fluorescence relaxation in dark adapted leaves of WT and Δ*rbcL* mutant, in the absence of DCMU, averaged from several experimental results. Despite a large variation in the kinetics of the flash-induced fluorescence decay detected from different leaves and even from different parts of the same leaf, the overall view was always the same—the reoxidation kinetics of flash-induced Q_A^- in mutant leaves was significantly slower than in WT leaves.

TL measurements performed on WT thylakoids showed the main B-band at 24 °C, which arises from recombination of Q_B^- at the acceptor side of PSII with the S_2 state of the water oxidising complex at the donor side. In Δ*rbcL* thylakoids, the peak position of the main TL-band was shifted from 24 °C to 19 °C (Fig. 3C) indicating a destabilisation of the $S_2Q_B^-$ charge pair. This effect was further supported by the TL measurements performed on leaf segments also showing the downshift of the peak position of the B-band from about 40 °C to 35 °C (data not shown). In the presence of DCMU, the main TL band (Q-band), which arises from the $S_2Q_A^-$ recombination, was not affected by mutation (Fig. 3C, shown as inset). Since the same S_2 state participates in the destabilised $S_2Q_B^-$ and in the unaffected $S_2Q_A^-$ recombination, we can conclude that the mutation does not affect the redox properties of the S_2 state and of Q_A, but leads to the destabilisation of Q_B. It is noteworthy to point out the slightly modified shape of the TL-glow curve in Δ*rbcL* thylakoids, in the absence of DCMU (Fig. 3C). The appearance of a small bump at around 10 °C, at the same temperature as the Q-band, can indicate about the presence of small component of Q-band hidden under the main TL-curve in the absence of DCMU in Δ*rbcL* mutant thylakoids.

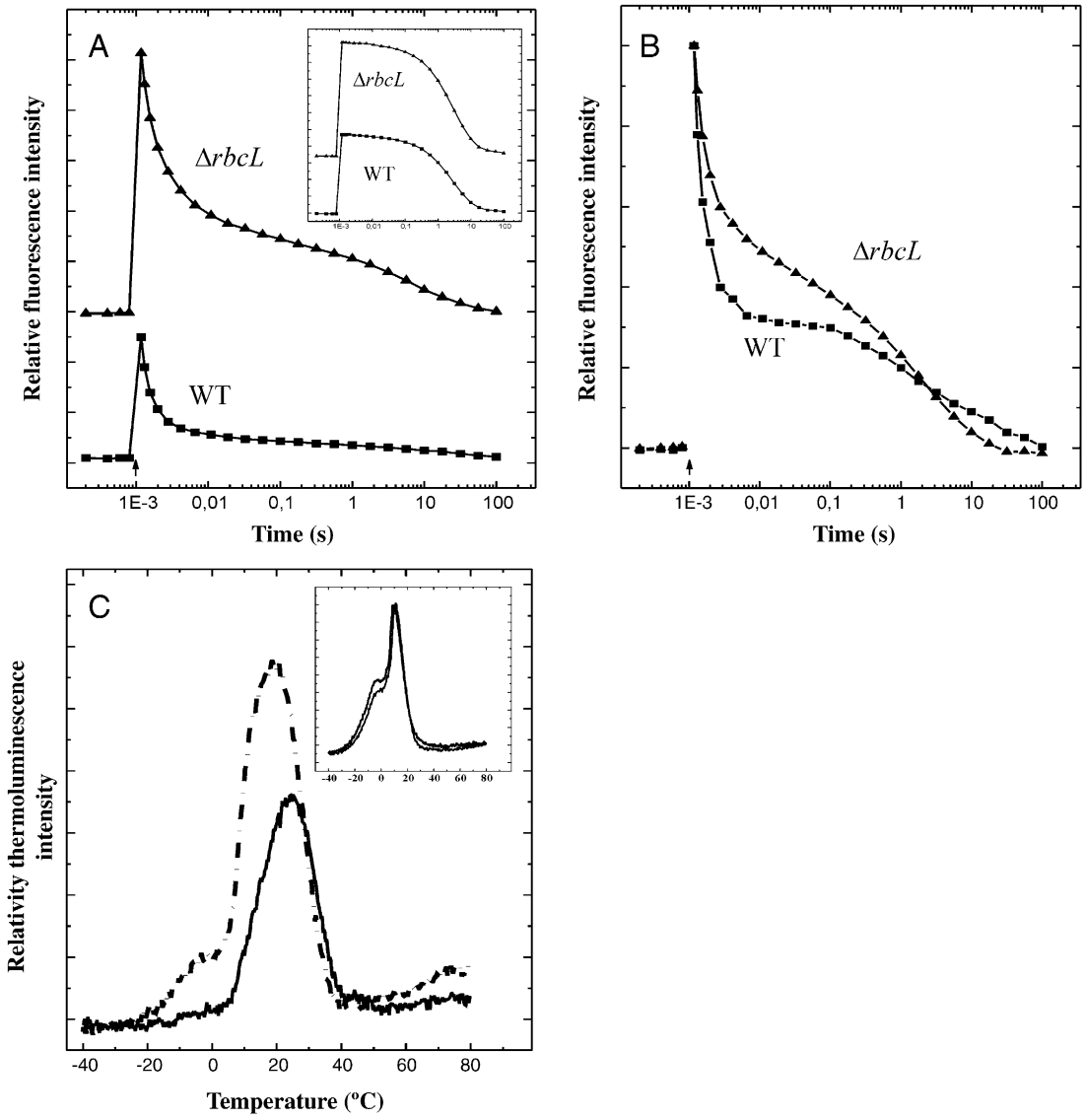

Fig. 3. Comparison of PSII electron transport properties of the WT and Δ*rbcL* plants. (A) Relaxation of the flash-induced fluorescence yield in WT (■) and Δ*rbcL* (▼) thylakoids. The inset shows the flash-induced variable fluorescence relaxation measured in the presence of 10 μM DCMU. (B) Relaxation of flash-induced fluorescence yield in WT (■) and Δ*rbcL* (▼) leaf discs. The traces are the averages of several recordings. For easy comparison, the fluorescence relaxation curves were normalized to the same amplitude. (C) TL characteristics of WT (solid line) and Δ*rbcL* (dotted line) thylakoids. Samples were excited with one flash either at +5 °C in the absence or −10 °C in the presence of 10 μM DCMU (shown as inset).

The light saturated steady-state oxygen evolution measurements with WT and mutant thylakoids exhibited maximum rates of 121 and 99 μmol O_2 mg^{-1} Chl h^{-1}, respectively (Table 2).

3.4. The effect of ΔrbcL mutation on PSI function

PSI photochemical activity in WT and Δ*rbcL* thylakoids was measured using the kinetic traces of the flash-induced

Table 1
Characteristics of flash-induced chlorophyll fluorescence relaxation in the WT and Δ*rbcL* mutant thylakoids

	Total amp (%)	Fast phase τ/Amp (ms)/(%)	Middle phase τ/Amp (ms)/(%)	Slow phase τ/Amp (s)/(%)
No addition				
WT	100	0.63±0.06/65±2	22.1±0.5/16±1	9.3±2.1/19±0.8
Δ*rbcL*	100	1.12±0.01/42±2	29.6±0.01/19±1	5.9±0.05/39±2
With DCMU				
WT	100	12.6±0.01/1.4±0.15	−/0	4.0±0.05/98.6±2
Δ*rbcL*	100	12.5±0.01/1.4±0.11	−/0	4.0±0.12/98.6±3

Numbers represent mean of four measurements±S.E. Values are relative amplitudes in percent of total variable fluorescence obtained after the fired flash.

Table 2
Comparison of photosynthetic activity of PSII and PSI complexes in WT and Δ*rbcL* tobacco thylakoids

	PSII (μmol O_2 mg Chl^{-1} h^{-1})/(%)[a]	PSI P700 arb.u. (%)[a]
Control		
WT	121/(100%)	100
Δ*rbcL*	99/(81%)	62
High light		
WT	97/(80%)	98
Δ*rbcL*	60/(61%)	75

Steady-state rates of oxygen evolution measured in the presence of 1 mM DMBQ as artificial electron acceptor.
[a] Numbers in parentheses mean percent of the particular parameter taking value in WT as 100%, except for high light treated Δ*rbcL* mutant, for which Δ*rbcL* control was taken as 100%.

absorbance changes around 820 nm (Fig. 4). The maximum level of photooxidisible P700 in Δ*rbcL*, measured by excitation of the samples with laser flash, was significantly lower than that in the WT samples.

The rate of $P700^+$ reduction in darkness was likewise slower in the Δ*rbcL* thylakoids than in WT suggesting poor electron supply from the intersystem chain to oxidised P700. In the presence of artificial electron donor (2,6-dichlorophenol indophenol and ascorbate), this difference between WT and Δ*rbcL* thylakoids was abolished (data not shown).

Considering the observed large variable fluorescence and the large amplitude of TL B-band in the mutant thylakoids (Fig. 3), and a lower amount of flash-induced photo-oxidisible P700 (Fig. 4), it can be concluded that the PSI/PSII ratio in Δ*rbcL* plants was lower than in WT. By using room temperature EPR measurements of the dark stable $Y_D^{\cdot}$ radical and the $P700^+$, recorded from the ferricyanide-oxidised samples, we obtained the values of 0.94 and 0.41 for the PSI/PSII ratios in WT and Δ*rbcL* thylakoids, respectively (Fig. 5).

3.5. 77K fluorescence emission spectrum

WT thylakoids showed typical 77 K fluorescence emission spectrum with 685, 695 and 733 nm fluorescence peaks (Fig. 6). It is well documented that the CP43 and CP47 inner antenna complexes of PSII give rise to the 685- and 695-nm fluorescence emission peaks, respectively, whereas the 733-nm fluorescence emission peak belongs to PSI complex [30]. The 77 K fluorescence emission spectrum of Δ*rbcL* thylakoids revealed a band at 680 nm (Fig. 6), implying the presence of free LHCII. This is in line with the fluorescence characteristics of PSII, always showing a high F_0 level in the Δ*rbcL* thylakoids (Fig. 3A). Moreover, it is noteworthy that illumination with far-red light or long dark adaptation of plants did not reduce the high F_0 level (data not shown). A blue shift from the emission maximum at 733 nm to 730 nm was also observed in the 77 K emission spectrum of mutant thylakoids, which suggested that the interaction between LHCI and PSI core was affected in the Δ*rbcL* plants.

3.6. Chlororespiratory electron transfer in ΔrbcL plant

Illumination of WT leaves with white actinic light for a few minutes followed by switching off the light, lead to a rapid transient 'dark rise' of F_0 chlorophyll fluorescence (Fig. 7). This 'dark rise' of F_0 chlorophyll fluorescence has been interpreted as an indicator of dark reduction of the plastoquinone (PQ) pool by stromal reductants [31]. As shown in Fig. 7, the Δ*rbcL* plants lacked the transient 'dark rise' of F_0 after turning off the actinic light.

3.7. Sensitivity of ΔrbcL plants to high light

After 2 h of high light illumination (1000 μmol photons m^{-2} s^{-1}) of the plants, the rate of steady state oxygen evolution, measured in the presence DMBQ, was inhibited 20% in WT and 39% in the thylakoids isolated from WT and Δ*rbcL* plants, respectively (Table 2), indicating a somewhat higher susceptibility of the Δ*rbcL*PSII complex to high light irradiance than of the WT PSII.

Similarly, in thylakoids isolated from high light treated Δ*rbcL* plants, the slow down of the flash-induced fluorescence relaxation kinetic was much more prominent than in WT (Fig. 8A, shown as inset). Also, the decrease in the amplitude of the total fluorescence was much more

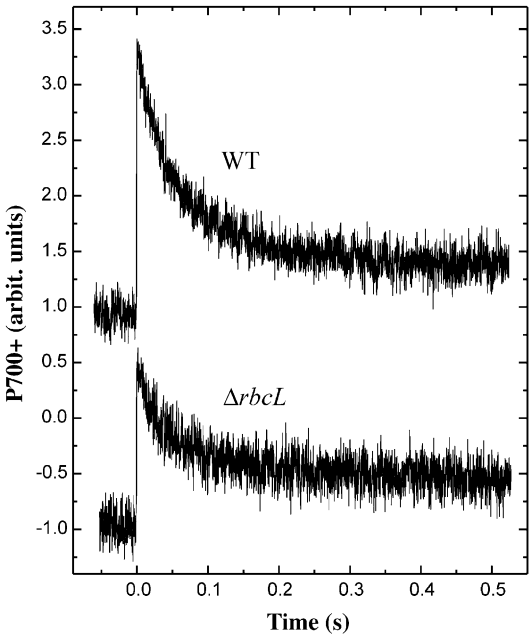

Fig. 4. Kinetic traces of P700 oxido-reduction in WT and Δ*rbcL* tobacco plants. Oxido-reduction of $P700^+$ in isolated thylakoids of WT and Δ*rbcL* mutant.

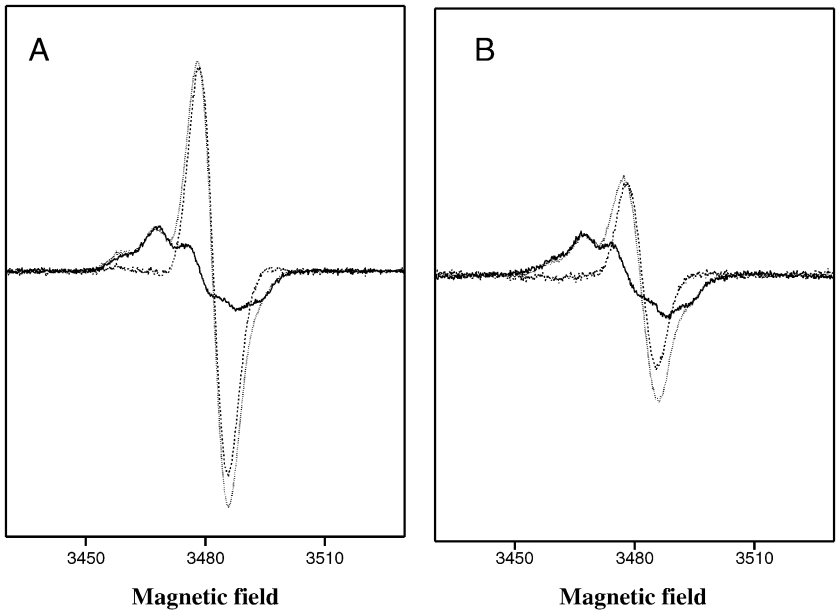

Fig. 5. EPR spectra recorded from WT (A) and Δ*rbcL* (B) thylakoid membranes. EPR spectra recorded in the dark after illumination of sample that fully oxidised Y_D from PSII (1 spin per PSII reaction center, solid line) and after oxidation of sample with 5 mM ferricyanide, representing both oxidised $Y_D^{\bullet}$ and $P700^+$ radicals (dotted line) and ferricyanide oxidised minus dark difference spectra representing pure $P700^+$ (1 spin per PSI, dashed line). The EPR conditions: room temperature, microwave frequency 9.78 GHz, microwave power 8 mW, modulation amplitude 5 G.

pronounced in the Δ*rbcL* mutant than in WT (Fig. 8A). There is a risk of under-estimation of the total fluorescence amplitude in nontreated WT thylakoids due to a possible loss of the very fast signal points of the fluorescence relaxation curve, and therefore, the relaxation curves monitored in the presence of DCMU were used to compare the total fluorescence amplitude, which decreased from 100% to 75% and 38% in high light illuminated (300 μmol photons m^{-2} s^{-1}, 4 h) WT and Δ*rbcL* thylakoids, respectively, but no difference in the relaxation kinetics was observed (data not shown).

As depicted in Fig. 8B, the intensity of the TL B-band in thylakoids isolated from photoinhibited WT decreased to a

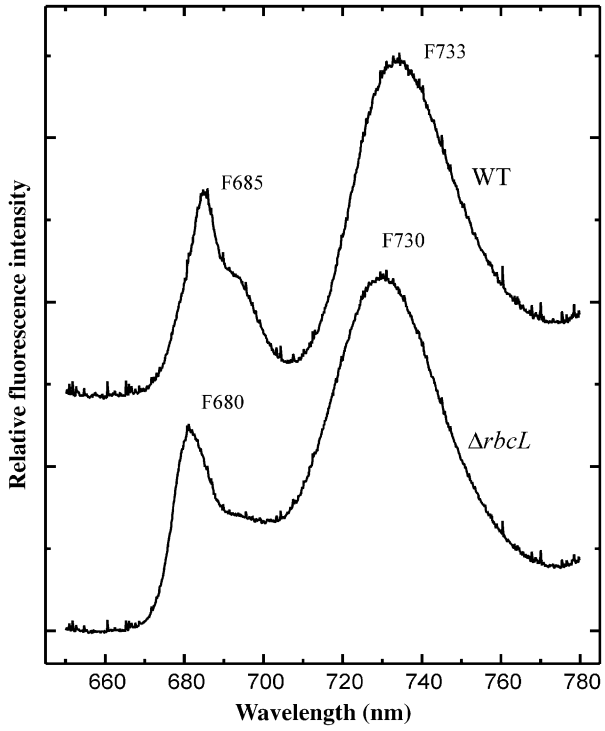

Fig. 6. Chlorophyll fluorescence emission spectra recorded at 77 K from WT and Δ*rbcL* thylakoids. Excitation of Chl *a* was below 500 nm.

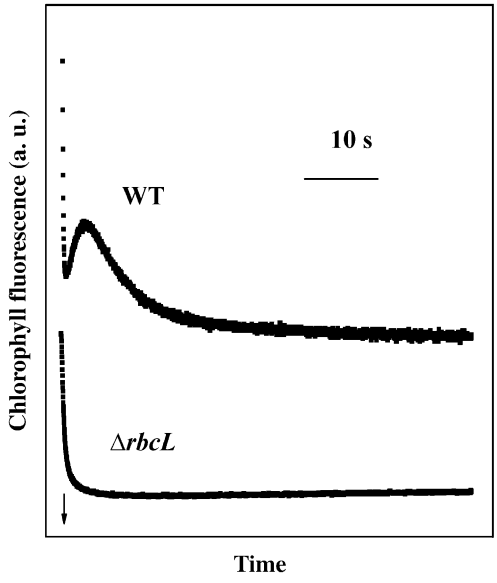

Fig. 7. Dark 'F_0 rise' of chlorophyll fluorescence upon a light to dark transition in WT and Δ*rbcL* leaves. F_0 'rise' was recorded after actinic light (100 μmol photons m^{-2} s^{-1}) has been switched off. Downward pointing arrow indicates switching off actinic light.

smaller extent than in the Δ*rbcL* thylakoids, which is in accordance with fluorescence relaxation measurements. Similar results were obtained also with the TL Q-band (data not shown).

Interestingly, when the photoinhibition experiments were performed with isolated thylakoids, the 50-min exposure of WT thylakoids to high light resulted in the modification of fluorescence relaxation kinetics being very similar to that recorded in nontreated Δ*rbcL* thylakoids (0 min photoinhibition) (Fig. 8C). Such overlapping of the decay curves confirms that the Δ*rbcL* plants suffer from chronic photoinhibition even under growth light condition of only 10 μmol photons m^{-2} s^{-1}.

The amount of photooxidisible P700 during the 2-h illumination of the plants with 1000 μmol photons m^{-2} s^{-1} was practically unchanged in WT, but decreased to 75% in Δ*rbcL* mutant (Table 2).

Since the inhibition of PSI has been inferred to result from producing of ROS, the H_2O_2 accumulation in high light treated leaves was tested by using the DAB-staining method. The leaf discs cut off from high light treated WT leaves revealed only very small amount of DAB-detectable H_2O_2 accumulation. On the contrary, massive accumulation of H_2O_2 in high light treated Δ*rbcL* leaves was visualised from the reddish-brown colored precipitants of oxidised DAB (Fig. 8D).

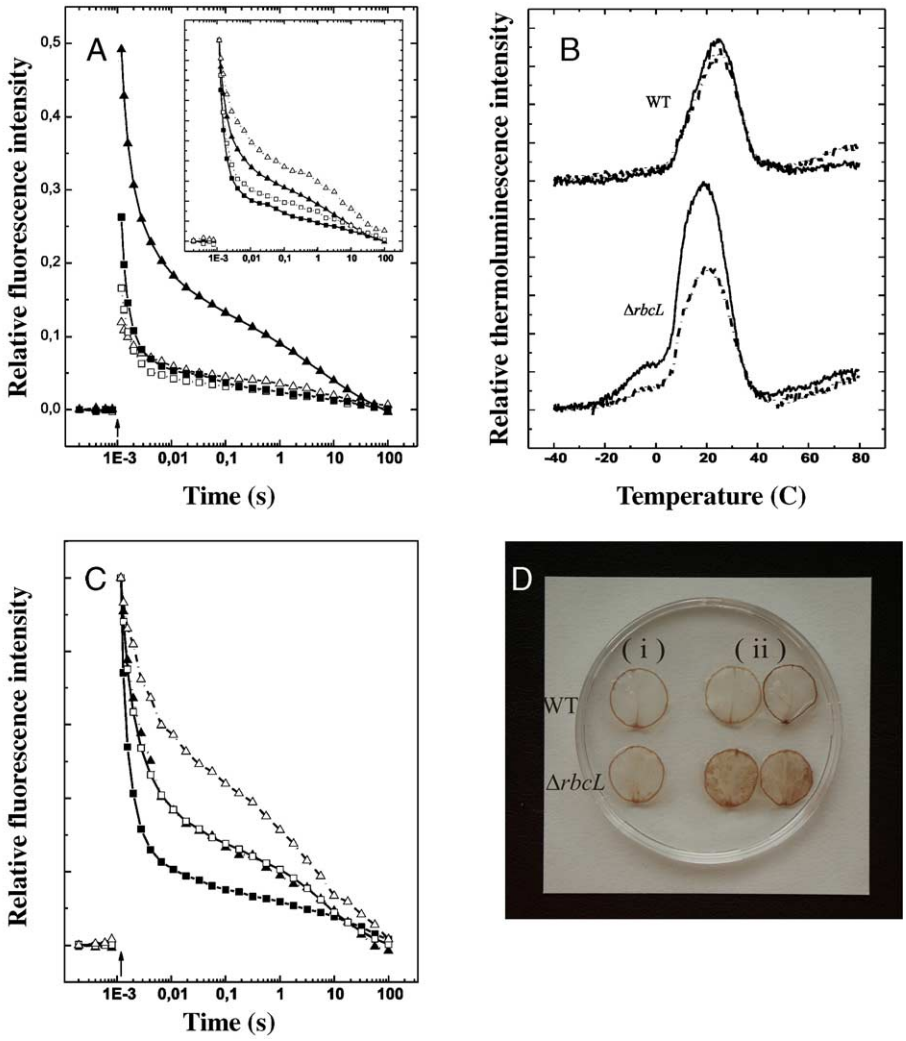

Fig. 8. Effect of high light illumination on the WT and Δ*rbcL* thylakoids. (A) The effect of high light illumination on the relaxation of flash-induced variable fluorescence. Plants were illuminated at 1000 μmol photons m^{-2} s^{-1} for 2 h and the flash-induced fluorescence relaxation detected from isolated thylakoids; (■)—nontreated WT, (□)—high light treated WT, (▼)—nontreated Δ*rbcL*, (Δ) high light treated mutant. (B) The effect of high light illumination on the TL characteristics of the WT and Δ*rbcL* thylakoids isolated from treated plants. Solid line—nontreated samples, dotted line—photoinhibited plants. (C) Isolated thylakoids were exposed to white light at 300 μmol photons m^{-2} s^{-1} intensity for 0 (filled symbols) and 50 min (open symbols) and flash-induced fluorescence relaxation was detected after 5 min dark adaptation. (■)—nontreated WT, (□)—high light treated WT, (▲)—nontreated Δ*rbcL*, (Δ) high light treated mutant. The curves are normalized to the same amplitude for easy comparison. (D) H_2O_2 accumulation in the leaf discs from WT and Δ*rbcL* plants. The H_2O_2 accumulation was detected by immersing the treated leaves in DAB solution. (i) leaves were treated at 250 μmol photons m^{-2} s^{-1} for 30 min, (ii) leaves were treated at 1000 μmol photons m^{-2} s^{-1} for 1 h.

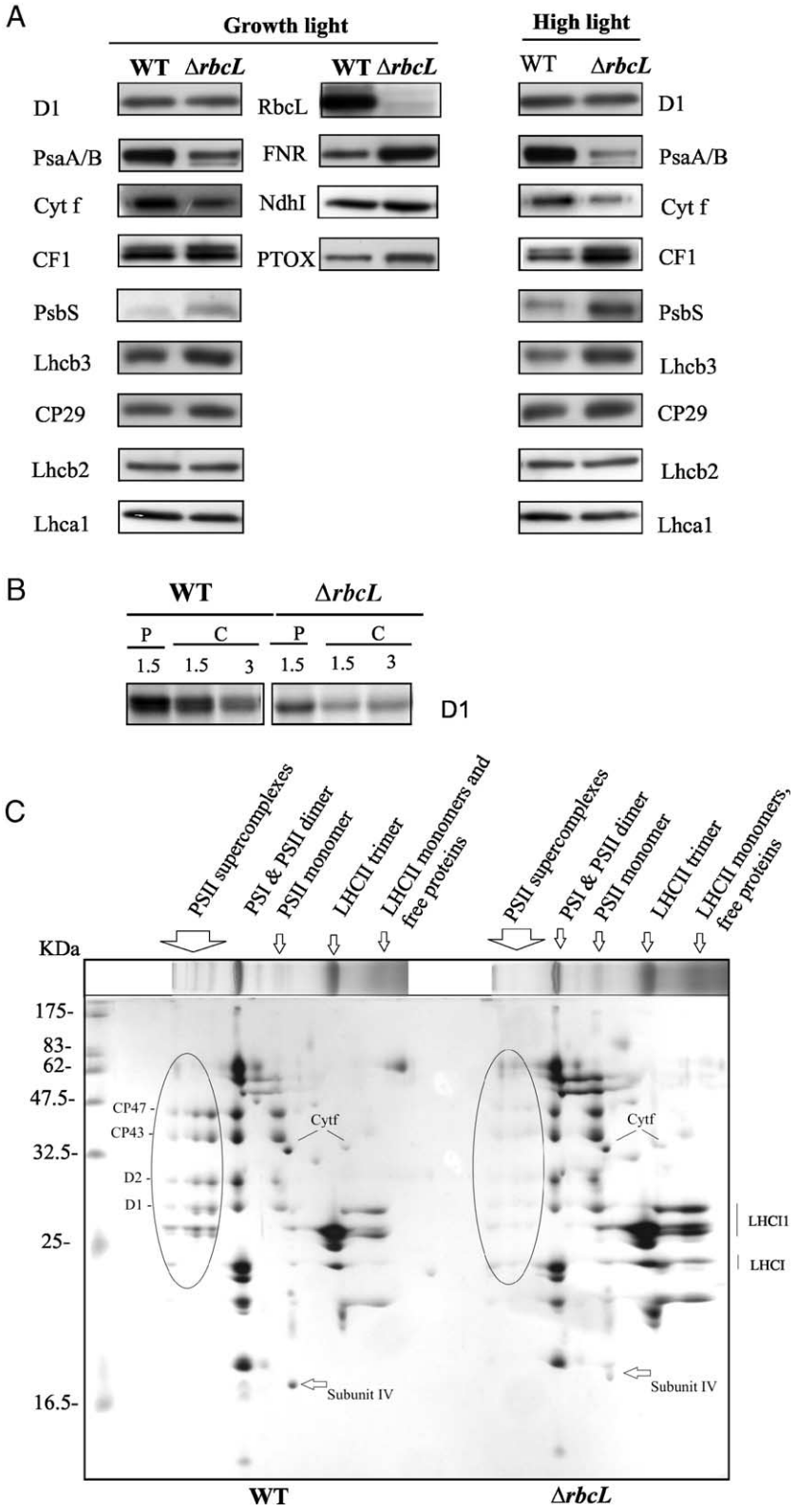

Fig. 9. Biochemical analysis of WT and Δ*rbcL* thylakoid membranes and protein extracts. (A) Immunoblots of the thylakoid membranes and protein extracts obtained from nontreated plants (left and middle panel) and from the plants treated for 2 h under 1000 μmol photons m^{-2} s^{-1} (right panel). All samples were loaded on a Chl basis (0.3 μg Chl per line, except for Ndh I, PTOX 8 and 3 μg Chl, respectively), (B) An autoradiogram showing the in vivo ^{35}S Met-labeled D1 protein pulse for 1.5 h (P) and subsequent chase for 1.5 and 3 h. (C) Silver-stained gel showing the distribution of protein complexes and their subunit composition in WT and Δ*rbcL* thylakoid membranes after 2D-BN-PAGE/SDS-PAGE separation. For more detailed description of protein identification, see Ref. [51].

3.8. Thylakoid polypeptide composition and turnover of the D1 protein

Immunoblot analysis of the thylakoid membrane and stromal proteins from WT and Δ*rbcL* leaves are shown in Fig. 9A. The amount of D1, the PSII reaction center protein, was about 91% in mutant thylakoids, compared with WT. The levels of PSI-PsaA/B proteins and Cytochrome (Cyt) f were more pronouncedly reduced to, 62% and 55%, respectively, in the mutant thylakoids as compared to WT, whereas a higher amount of CF1 subunit of ATP-synthase was recorded, compared with the WT thylakoids (Fig. 9A, left panel).

The relative amounts of PsbS, Lhcb3, and CP29 in mutant thylakoids were found to be significantly higher, whereas Lhca1 was slightly downregulated as compared to WT. All other examined Lhcb and Lhca proteins were almost of similar quantity in the thylakoids of the Δ*rbcL* and WT tobacco plants.

Interestingly, the quantitative analysis of thylakoids and leaf extracts revealed that the Δ*rbcL* mutant had dramatically elevated amounts of Ferredoxin-NADP oxidoreductase (FNR) compared to WT. In the Δ*rbcL* thylakoids the contents of plastid-terminal oxidase (PTOX) and the Ndh-I subunit of the NDH-1 complex, involved in chlororespiration, were about 210% and 130% of that in WT (Fig. 9A, middle panel).

Similar protein analysis was performed on thylakoids isolated from high light illuminated WT and Δ*rbcL* plants. As depicted in Fig. 9A (right panel), the steady state D1 protein level in high light treated Δ*rbcL* plants was reduced only slightly more than in WT. Much more dramatic decreases as compared to WT were observed in protein levels of PsaA/B and Cyt f in Δ*rbcL* thylakoids isolated from high light treated plants. On the contrary, the Δ*rbcL* thylakoids revealed significantly stronger accumulation of PsbS, Lhcb3 and CP29 during the high light treatment of plants as compared to WT.

Due to photoinhibition of both PSI and PSII, and the accumulation of ROS in the Δ*rbcL* plants in high light, we performed in vivo ^{35}S Met pulse-chase experiment to clarify whether the D1 protein is still capable of turn-over in high light. As shown in Fig. 9B, the accumulation of ^{35}S Met in the D1 protein during the 1.5 h pulse at growth light conditions was more rigorous in WT than in Δ*rbcL* plants. During the chase at PFD of 500 μmol photons m^{-2} s^{-1}, a rapid D1 protein degradation occurred in WT thylakoids, as can be deduced from Fig. 9B. Also the Δ*rbcL* mutant showed D1 protein degradation during chase experiments. Taken together, both the synthesis and degradation of the D1 protein in Δ*rbcL* plants, although evident, were somewhat slowed down as compared to WT plants. Also, a slightly slower recovery from photoinhibition was recorded in mutant plants when the recovery of PSII activity was monitored by oxygen evolution measurements in WT and Δ*rbcL* mutant plants (data not shown).

2D-BN/SDS-PAGE experiments demonstrated the lack of PSII supercomplexes and a relatively higher amount of free LHCII and LHCI proteins in Δ*rbcL* thylakoids compared to WT (Fig. 9C). The mutant thylakoids were also characterized by a low amount of PSII dimers and a higher amount of PSII monomers.

4. Discussion

A transplastomic tobacco line with deleted *rbcL* gene was used to investigate the acclimation of the thylakoid components to conditions of a deficiency of terminal electron acceptors of photosynthetic light reactions. To this end, the Δ*rbcL* and WT plants were comparatively analyzed with regard to the functional and structural states of PSII and PSI, by focusing on the relationship and interaction of the two photosystems both under growth light and after a short exposure to high light.

4.1. ΔrbcL mutation induces acceptor side modifications of PSII without any detrimental donor side effect

In the Δ*rbcL* thylakoids the relaxation of flash-induced fluorescence was characterized by significantly slower time constant and decreased relative amplitude of the fast phase as compared to WT (Fig. 2, Table 1). This clearly indicates a modification in the forward electron transfer from Q_A^- to Q_B (Q_B^-) and is likely to result in an increased population of reduced Q_A^- in Δ*rbcL* PSII reaction centers. It is interesting to note that concomitantly with a slower middle phase in the Δ*rbcL* thylakoids, which indicates a slow rebinding of PQ, an increase in the relative amplitude of this phase was also evident. This, in turn, shows that in the mutant more of the PSII reaction centers had an empty Q_B pocket in darkness at the moment of flashing as compared to WT. These results, together with the dramatically increased relative amplitude of the slow phase in Δ*rbcL* mutant thylakoids, strongly suggest that the PQ pool is limited/reduced and recombination of $(Q_AQ_B)^-$ with the donor side components becomes dominating in the mutant thylakoids. In the Δ*rbcL* thylakoids, the time constant of the slow phase of the flash fluorescence relaxation did not noticeably differ whether the curves were recorded in the absence or presence of DCMU (Table 1). This slow component of the fluorescence relaxation curve, in the absence of DCMU, arises from $S_2/(Q_AQ_B)^-$ recombination, whereas in the presence of DCMU the slow decay phase comes from the $S_2Q_A^-$ recombination. These fluorescence results, together with TL measurements showing a downshift of the peak temperature of the B-band and also existence of the some components of the residual Q-band even in the absence of DCMU (Fig. 3B), suggest a decreased equilibrium constant for sharing an electron between Q_A and Q_B in the Δ*rbcL* thylakoids.

Analysis of the higher organisation of PSII complexes by 2D-BN/SDS-PAGE, on the other hand, revealed in Δ*rbcL*

thylakoids mostly PSII monomer complexes, which have been characterized by slow electron transfer on the acceptor side of PSII and being located in stroma lamellae [32]. Although we cannot completely exclude the possibility that the PSII centers in Δ*rbcL* mutant resemble PSIIs of stroma lamellae, not even traces of PSII centers lacking the bound Mn cluster [32] could be identified in Δ*rbcL* thylakoids; indeed, the flash-induced fluorescence relaxation in the presence of DCMU did not show any fast phase typical to PSIIs in the stroma lamellae fraction.

Modified acceptor side of PSII in Δ*rbcL* could result from an altered Q_B binding site. However, DCMU was effective in blocking the Q_A to Q_B electron transfer in the mutant thylakoids. Moreover, the flash-induced fluorescence relaxation measurements performed in the presence of an artificial electron acceptor, DMBQ, modified the fluorescence relaxation kinetics in the WT and the Δ*rbcL* mutant to similar extent (data not shown). Therefore, the modified acceptor side of PSII in Δ*rbcL* is likely due to alteration in the redox properties of Q_B and any serious structural changes inducing binding modifications in the Q_B pocket can be excluded.

Another characteristic feature of the Δ*rbcL* tobacco is a high level of minimum fluorescence F_0 and high amplitude of the variable fluorescence. High F_0 observed in the Δ*rbcL* mutant may indicate accumulation of free LHCII, which was confirmed by 77 K fluorescence emission experiments revealing an emission peak at 680 nm only in the mutant thylakoids (Fig. 6). The larger variable fluorescence detected from mutant plants would suggest that the Δ*rbcL* plants have more functional PSII capable of reducing the primary PSII acceptor Q_A. This interpretation, however, apparently contradicts the somewhat lower amounts of PSII core proteins in Δ*rbcL* thylakoids compared to WT, and therefore the reason for large variable fluorescence and high amplitude of TL B-band in Δ*rbcL* is not completely clear.

4.2. High NPQ of the ΔrbcL mutant is crucial for protecting the photosynthetic apparatus

Under continuous illumination conditions, the development of high NPQ in the Δ*rbcL* plants indicates enhanced dissipation of absorbed light energy as heat, thus, directing only a small fraction of absorbed light to photosystems. The major component of NPQ is energy-dependent component-qE, which requires *trans*-thylakoid pH gradient and shows fast relaxation kinetics (reviewed in [28,33]). The relative contribution of qE to overall NPQ seems to be dominating in both WT and Δ*rbcL* mutant leaves. The high steady-state value of NPQ in Δ*rbcL* plants was accompanied by an upregulation of PsbS. A close relation between qE and PsbS is a well-known phenomenon [34–36], although the functional mechanism of PsbS is not yet fully understood. It has been suggested that PsbS acts as a sensor, accepting excess excitation energy and dissipating it as heat or is involved in the modulation of LHCII and triggering it into a state of quenching. It is noteworthy that under high light treatment even more significant upregulation of PsbS occurred in Δ*rbcL* plants than in WT.

The Δ*rbcL* plants were characterized also by a high level of Lhcb3 and CP29, although one would have expected the mutant plants to reduce the chlorophyll antenna size in order to avoid excess absorption of light energy under limitation of terminal electron consumers. It is therefore conceivable that both CP29 and LHCII bind zeaxanthin in a pH-dependent way, being in line with an earlier observation suggesting that these Lhcb proteins can function as quenching sites [37]. The strong similarities in the kinetics during the formation of qE in intact chloroplasts and the quenching in the LHCII monomers and trimers, as well as in CP26 and CP29 also support this suggestion [38,39].

The development of large NPQ in the Δ*rbcL* plants (Fig. 2B) was accompanied by a decrease of photochemical quenching (data not shown) and ETR (Fig. 2A). The about 4-fold lower ETR suggests that the Δ*rbcL* plants are capable of considerable downregulation of the whole photosynthetic electron transport with upregulation of NPQ.

4.3. ΔrbcL mutant acquired several protection mechanisms against PSI-mediated ROS production

PSI is a potentially dangerous ROS generator, which may exert damage not only to PSI, but also to the PSII complex [11]. In the Δ*rbcL* mutant, the limitation of main photosynthetic electron consumers can induce strong excitation pressure on PSI even at low light, which in turn results in donation of electrons to molecular oxygen with concomitant production of highly dangerous ROS [40]. It is evident that the Δ*rbcL* plants have adopted several mechanisms to avoid PSI-mediated ROS production. (i) A significant downregulation of PSI contents in Δ*rbcL* thylakoids reveals an acclimation strategy of the photosynthetic apparatus known to occur at high light [41,42]. In addition to the lower amount of photooxidisible P700 as compared to WT, the Δ*rbcL* plants also had a lower PSI/PSII ratio as compared to WT. (ii) The 77 K fluorescence emission spectra showing a 3-nm blue shift in the peak position of PSI fluorescence and the 2D-gel analysis demonstrating free LHCI proteins suggest an impaired interaction between LHCI and the PSI core in the Δ*rbcL* mutant, thereby reducing PSI excitation [43]. (iii) Δ*rbcL* plants also showed slower re-reduction of $P700^+$ in darkness, implying decreased conductance of electron transport chain between PSII and PSI. (iv) Suppression of PSI mediated ROS production is likely contributed by an increased level of PTOX, a chlororespiratory component, evident in the thylakoid membrane of the Δ*rbcL* mutant. The redox status of the PQ pool in the dark depends on the equilibrium between NDH-1 and PTOX activity [44,45], and it is therefore conceivable that a more strongly upregulated PTOX in Δ*rbcL* thylakoids functions as an electron sink in the intersystem chain. The absence

of the transient 'dark rise' of F_0 chlorophyll fluorescence, as we observed in Δ*rbcL* plants, has been previously detected in Ndh deficient mutant plants [16,46,47] and also in transgenic tobacco plants constitutively overexpressing At-PTOX [46]. Upregulated PTOX in the Δ*rbcL* mutant is likely to play a dual role also in the light, on one hand by preventing electron flow to PSI and thus protecting PSI against photodamage and on the other hand by functioning as a co-factor in the early stages of carotenoid desaturation [48,49].

4.4. High light illumination of the ΔrbcL mutant damages both the PSI and PSII complexes

It is conceivable from the above characterization of the Δ*rbcL* tobacco mutant that under very low growth light conditions, they use acclimation strategies typical to WT plants only under chilling conditions in moderate light [9,11,50]. These strategies include down regulation of linear electron flow, decreasing PSI/PSII ratio and turning on the protective mechanisms, which include the upregulation of NPQ, upregulation of alternative electron sinks and most probably also an accumulation of reasonable amounts of enzymes scavenging ROS and other harmful compounds. Upon sudden increase in light intensity, however, the rate of PSII photodamage exceeds the rate of de novo D1 synthesis due to the fact that PSII and its antenna are no more able to downregulate excess absorbed energy by NPQ, resulting in a decrease of the photochemical efficiency of PSII both in the WT and Δ*rbcL* thylakoids. Loss of PSII reaction center proteins, however, was not more severe in the Δ*rbcL* than in WT thylakoids. In sharp contrast to PSII, the PSI reaction centers of only the Δ*rbcL* mutant suffered from high light exposure of plants, showing a considerable loss of photo-oxidisible P700. Sensitivity of Δ*rbcL* PSI complex to high light was even more drastically demonstrated by a loss of PSI reaction center proteins, and also of the Cytf subunit of the Cytbf complex. This was most likely a consequence of production of ROS in Δ*rbcL* PSI centers generated at high light when the quenching capacity in the thylakoid membrane was exhausted (Fig. 8D). Severe response of Δ*rbcL* PSI complex to high light thus emphasises a crucial role of thylakoid quenching systems, most probably including the down regulation of PSII, in the protection of PSI from photodamage.

Under physiological growth temperatures, the PSI complex is generally protected against photodamage because of possibilities for efficient development of excitation energy quenching. High light acclimation, however, results in controlled PSI degradation, possibly via ROS produced in PSI centers themselves. Finally, when all quenching and acclimation strategies are exhausted, as in Δ*rbcL* mutant at high light, or when their development is prevented, for example at low temperature, the PSI centers become the primary targets of photodamage of the photosynthetic apparatus.

In summary, based on fluorescence relaxation and TL measurements, we conclude that the deletion of *rbcL* leads to a modification of the acceptor side of PSII at the level of Q_A to Q_B electron transfer. Judged from the protein contents, photosynthetic activity measurements, and EPR spectroscopy, it is evident that Δ*rbcL* mutation leads to a decrease in the PSI/PSII ratio. Moreover, the flexibility of PSII plays a crucial role in protection of both photosystems against irreversible protein damages when terminal electron acceptors are limited. High level of NPQ in Δ*rbcL* plants is able to dissipate significant amount of absorbed light energy with a concomitant decrease in linear electron transport. Modifications of the photosynthetic pigment–protein complexes and other interacting thylakoid proteins in Δ*rbcL* mutant are probably a result of acclimation to limited electron sinks, thereby allowing the survival of the Δ*rbcL* plants under growth light condition. Indeed, an extra high light stress induced a severe degradation of PSI in Δ*rbcL* plants.

Further investigations of all photoprotective mechanisms, together with other structural adaptation processes, will make the Rubisco-less tobacco mutant a good model for resolving photoinhibition-related mechanism(s) in vivo occurring under the limitation of terminal electron acceptors.

Acknowledgements

This study was financially supported by the grant from the Academy of Finland and the Finnish Ministry of Agriculture (NKJ project) and also partly supported by the CIMO bilateral grant between the laboratories of E-M.A. and I.V., by grants from the Hungarian Granting Agency, OTKA (T034321), and from the European Union (MRTN-CT-2003-505069). F.M. acknowledges financial support from the Swedish Research Council. We thank Dr. A. Krieger-Liszkay for critical reading of manuscript, Prof. S. Styring for useful discussion, Ms. Virpi Paakkarinen and Mr. Mika Keränen for excellent technical assistance. We are grateful to Prof. P. Maliga for providing us with Δ*rbcL* mutant seeds. We also thank Dr. T.Hundal (PSI and CF1), Dr. F.A. Wollman. (Cytf), Dr. M. Wentworth (PsbS), Dr. S. Jansson (CP29), Dr. H.V. Scheller (FNR), Dr. P. Nixon (NdhI) and Ms. D. Martinez (RbcL) for their kind gift of the antibodies.

References

[1] H.M. Miziorko, G.H. Lorimer, Ribulose-1,5-biphosphate carboxylase-oxygenase, Annu. Rev. Biochem. 52 (1983) 507–535.
[2] I. Kanevski, P. Maliga, Relocation of the plastid *rbcL* gene to the nucleus yields functional ribulose-1,5-bisphosphate carboxylase in tobacco chloroplasts, Proc. Natl. Acad. Sci. U. S. A. 91 (1994) 1969–1973.
[3] B. Kok, E.B. Gassner, H.J. Rurainski, Photoinhibition of chloroplast reactions, Photochem. Photobiol. 2 (1966) 215–227.

[4] S.B. Powles, Photoinhibition of photosynthesis induced by visible light, Annu. Rev. Plant Physiol. 35 (1984) 15–44.
[5] E.-M. Aro, I. Virgin, B. Andersson, Photoinhibition of Photosystem II: inactivation, protein damage and turnover, Biochim. Biohys. Acta 1143 (1993) 113–134.
[6] I. Vass, S. Styring, T. Hundal, A. Koivuniemi, E.-M. Aro, B. Andersson, Reversible and irreversible intermediates during photoinhibition of photosystem II: stable reduced QA species promotes chlorophyll triplet formation, Proc. Natl. Acad. Sci. U. S. A. 89 (1992) 1408–1412.
[7] M. Havaux, A. Davaud, Photoinhibition of photosynthesis in chilled potato leaves is not correlated with a loss of Photosystem-II activity. Preferential inactivation of Photosystem I, Photosynth. Res. 40 (1994) 75–92.
[8] K. Sonoike, I. Terashima, M. Iwaki, S. Itoh, Destruction of photosystem I iron-sulfur centers in leaves of *Cucumis sativus* L. by weak illumination at chilling temperature, FEBS Lett. 362 (1995) 235–238.
[9] K. Sonoike, Degradation of *psaB* gene product, the reaction center subunit of photosystem I, is caused during photoinhibition of photosystem I: possible involvement of active oxygen species, Plant Sci. 115 (1996) 157–164.
[10] S.E. Tjus, B.L. Møller, H.V. Scheller, Photosystem I is an early target of photoinhibition in barley illuminated at chilling temperatures, Plant Physiol. 116 (1998) 755–764.
[11] S.E. Tjus, H.V. Scheller, B. Andersson, B.L. Møller, Active oxygen produced during selective excitation of Photosystem I is damaging not only to Photosystem I, but also to Photosystem II, Plant Physiol. 125 (2001) 2007–2015.
[12] K.K. Niyogi, Safety valves for photosynthesis, Curr. Opin. Plant Biol. 3 (2000) 455–560.
[13] B. Andersson, E.-M. Aro, Proteolytic activities and proteases of plant chloroplasts, Physiol. Plant. 100 (1997) 780–793.
[14] K. Asada, The water–water cycle in chloroplasts: scavenging of active oxygens and dissipation of excess photons, Annu. Rev. Plant Physiol. Plant Mol. Biol. 50 (1999) 601–639.
[15] A.L. Lee, J.P. Thornber, Analysis of the pigment stoichiometry of pigment–protein complexes from barley (*Hordeum vulgare*). The xanthophyll cycle intermediates occur mainly in the light-harvesting complexes of photosystem I and photosystem II, Plant Physiol. 107 (1995) 565–574.
[16] T. Endo, T. Shikanai, A. Takabayashi, K. Asada, F. Sato, The role of chloroplastic NAD(P)H dehydrogenase in photoprotection, FEBS Lett. 457 (1999) 5–8.
[17] Y. Munekage, M. Hojo, J. Meurer, T. Endo, M. Tasaka, T. Shikanai, PGR5 is involved in cyclic electron flow around Photosystem I and is essential for photoprotection in *Arabidopsis*, Cell 110 (2002) 361–371.
[18] T. Murashige, F. Skoog, A revised medium for rapid growth and bioassay with tobacco tissue cultures, Physiol. Plant. 15 (1962) 493–497.
[19] R.J. Porra, W.A. Thompson, P.E. Kriedemann, Determination of accurate extinction coefficients and simultaneous equations for assaying chlorophyll a and b with four different solvents: verification of the concentration of chlorophyll by atomic absorption spectroscopy, Biochim. Biophys. Acta 975 (1989) 384–394.
[20] I. Vass, D. Kirilovsky, A.L. Etienne, UV-B radiation-induced donor- and acceptor-side modifications of photosystem II in the cyanobacterium *Synechocystis* sp. PCC 6803, Biochemistry 39 (1999) 12786–12794.
[21] A. Joliot, P. Joliot, Etude cinètique de la reaction photochimique libèrant l'oxygène au cours de la photosynthèse, C.R. Acad. Sci. 258 (1964) 4622–4625.
[22] M. Keränen, E.-M. Aro, E. Tyystjärvi, Excitation–emission map as a tool in studies of photosynthetic pigment–protein complexes, Photosynthetica 37 (1999) 225–237.
[23] R. Danielsson, P.-Å. Albertsson, F. Mamedov, S. Styring, Quantification of photosystem I and II in different parts of the thylakoid membrane from spinach, Biochim. Biophys. Acta 1608 (2004) 53–61.
[24] U.K. Laemmli, Cleavage of structural proteins during the assembly of the head of bacteriophage T4, Nature 227 (1970) 680–685.
[25] M. Kugler, L. Jänsch, V. Kruft, U.K. Schmitz, H.-P. Braun, Analysis of the chloroplast protein complexes by blue-native polyacrylamide gel electrophoresis (BN-PAGE), Photosynth. Res. 53 (1997) 35–44.
[26] A. Rokka, M. Suorsa, A. Saleem, N. Battchikova, E.-M. Aro, Synthesis and assembly of thylakoid protein complexes. Multiple assembly steps of photosystem II, Biochem. J. 386 (2005) 1–10.
[27] D. Ren, H. Yang, S. Zhang, Cell death mediated by MAPK is associated with hydrogen peroxide production in *Arabidopsis*, J. Biol. Chem. 277 (2002) 559–565.
[28] P. Müller, X.-P. Li, K.K. Niyogi, Non-photochemical quenching. A response to excess light energy, Plant Physiol. 125 (2001) 1558–1566.
[29] I. Vass, E. Turcsányi, E. Touloupakis, D. Ghanotakis, V. Petrouleas, The mechanism of UV-A radiation-induced inhibition of Photosystem II electron transport studied by EPR and chlorophyll fluorescence, Biochemistry 41 (2002) 10200–10208.
[30] G.H. Krause, E. Weis, Chlorophyll fluorescence and photosynthesis: the basics, Annu. Rev. Plant Physiol. Mol. Biol. 42 (1991) 313–349.
[31] J. Mano, C. Miyake, U. Schreiber, K. Asada, Chlorophyll fluorescence and photosynthesis: the basics, Plant Cell Physiol. 36 (1995) 1589–1598.
[32] F. Mamedov, H. Stefansson, P.A. Albertsson, S. Styring, Photosystem II in different parts of the thylakoid membrane: a functional comparison between different domains, Biochemistry 34 (2000) 10478–10486.
[33] N.E. Holt, G.R. Fleming, K.K. Niyogi, Towards an understanding of the mechanism of nonphotochemical quenching in green plants, Biochemistry 43 (2004) 8281–8289.
[34] X.-P. Li, O. Bjorkman, C. Shih, A.R. Grossman, M. Rosenquist, S. Jansson, K.K. Niyogi, A pigment-binding protein essential for regulation of photosynthetic light harvesting, Nature 403 (2000) 391–395.
[35] X.-P. Li, A.M. Gilmore, S. Caffarri, R. Bassi, T. Golan, D. Kramer, K.K. Niyogi, Regulation of photosynthetic light harvesting involves intrathylakoid lumen pH sensing by the PsbS protein, J. Biol. Chem. 279 (2004) 22866–22874.
[36] R.B. Peterson, E.A. Havir, A nonphotochemical-quenching-deficient mutant of *Arabidopsis thaliana* possessing normal pigment composition and xanthophylls-cycle activity, Planta 210 (2000) 205–214.
[37] T. Morosinotto, R. Baronio, R. Bassi, Dynamics of chromophore binding to Lhc proteins in vivo and in vitro during operation of the xanthophylls cycle, J. Biol. Chem. 277 (2002) 36913–36920.
[38] A.V. Ruban, M. Wentworth, P. Horton, Kinetic analysis of non-photochemical quenching of chlorophyll fluorescence: I. Isolated chloroplasts, Biochemistry 40 (2001) 9896–9901.
[39] M. Wentworth, A.V. Ruban, P. Horton, Kinetic analysis of non-photochemical quenching of chlorophyll fluorescence. 2. Isolated light-harvesting complexes, Biochemistry 40 (2001) 9902–9908.
[40] E.F. Elstner, Oxygen activation and oxygen toxicity, Annu. Rev. Plant Physiol. 33 (1982) 73–96.
[41] Y. Fujita, A study on the dynamic features of photosystem stoichiometry: accomplishments and problems for future studies, Photosynth. Res. 20 (1997) 697–705.
[42] J.M. Anderson, W.S. Chow, Y.I. Park, L.A. Franklin, S.P.-A. Robinson, P.R. van Hasselt, Response of *Tradescantia albiflora* to growth irradiance: change versus changeability, Photosynth. Res. 67 (2001) 103–112.
[43] H.J. Hwang, J.-H. Kim, Y.-J. Eu, B.Y. Moon, S.H. Cho, C.-H. Lee, Photoinhibition of photosystem I is accelerated by dimethyldithiocarbamate, and inhibitor of superoxide dismutase, during light-chilling of spinach leaves, J. Photochem. Photobiol., B Biol. 73 (2004) 79–85.
[44] T. Joët, L. Cournac, G. Peltier, M. Havaux, Cyclic electron flow around photosystem I in C(3) plants. In vivo control by the redox state

of chloroplasts and involvement of the NADH-dehydrogenase complex, Plant Physiol. 128 (2002) 760–769.
[45] L.M. Casano, J.M. Zapata, M. Martín, B. Sabater, Chlororespiration and poising of cyclic electron transport. Plastoquinone as electron transporter between thylakoid NADH dehydrogenase and peroxidase, J. Biol. Chem. 275 (2000) 942–948.
[46] P.A. Burrows, L.A. Sazanov, Z. Svab, P. Maliga, P. Nixon, Identification of a functional respiratory complex in chloroplasts through analysis of tobacco mutants containing disrupted plastid *ndh* genes, EMBO J. 17 (1998) 868–876.
[47] Y. Munekage, M. Hashimoto, C. Miyake, K. Tomizawa, T. Endo, M. Tasaka, T. Shikanai, Cyclic electron flow around photosystem I is essential for photosynthesis, Nature 429 (2004) 579–582.
[48] P. Carol, M. Kuntz, A plastid terminal oxidase comes to light: implications for carotenoid biosynthesis and chlororespiration, Trends Plant Sci. 6 (2001) 31–36.
[49] M. Kuntz, Plastid terminal oxidase and its biological significance, Planta 218 (2004) 896–899.
[50] N.G. Bukhov, S. Govindachary, S. Rajagopal, D. Joly, R. Carpentier, Enhanced rates of $P700^{+}$ dark-reduction in leaves of *Cucumis sativus* L. photoinhibited at chilling temperature, Planta 218 (2004) 852–861.
[51] E.-M. Aro, M. Suorsa, A. Rokka, Y. Allahverdiyeva, V. Paakkarinen, A. Saleem, N. Battchikova, E. Rintamäki, Dynamics of Photosystem II: a proteomic approach to thylakoid protein complexes, J. Exp. Bot. 56 (2005) 347–356.